Supporting Information for:
Measuring the building envelope penetration factor for ambient nitrogen oxides

Haoran Zhao,[1] Elliott T. Gall,[2] Brent Stephens[1,*]

[1]Department of Civil, Architectural, and Environmental Engineering, Illinois Institute of Technology, Chicago, IL 60616, USA
[2]Department of Mechanical and Materials Engineering, Portland State University, Portland, OR 97201, USA

*Corresponding author:
Brent Stephens, Ph.D.
Department of Civil, Architectural, and Environmental Engineering
Illinois Institute of Technology
Alumni Memorial Hall 228E
3201 South Dearborn Street
Chicago, IL 60616
Phone: (312) 567-3629
Email: brent@iit.edu

Table of Contents

Supplemental Methods

Test apartment description

The test apartment is located on the 3rd floor of a 9-story dormitory building on the main campus of Illinois Institute of Technology in Chicago, IL. The building is located ~500 m west of I-90/94 and ~1.3 km east of US-41 (Lake Shore Drive). The apartment has a floor area of ~60 m^2 and volume of ~150 m^3. The interior walls are painted plaster and the exterior enclosure is painted concrete block walls with single-pane aluminum-framed windows at window-to-wall ratio of ~50:50. There is a central 100% recirculating air-handling unit that is connect to rigid sheet metal ductwork installed within the conditioned space, but it is not connected to any heating and cooling system. Sampling locations and injection sites for NO_x and CO_2 are shown in Figure S1.

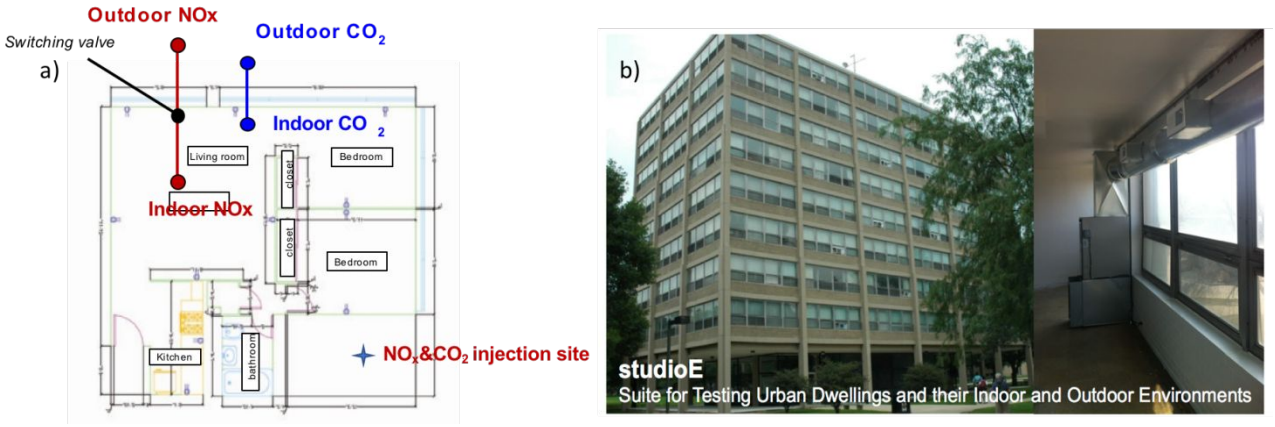

Figure S1. Description of (a) instruments set up indoors and (b) test apartment

Measurements of NO_2/NO/NO_x concentrations: Potential for interferences

Indoor and outdoor NO_2, NO, and total NO_x (NO + NO_2) concentrations were measured using a 2B Technologies Model 405 direct absorbance monitor. NO_2 is directly measured using absorbance at 405 nm, and NO is alternately measured by sequential conversion to NO_2 with internally generated ozone. Interference via photolysis of NO_2 due to 405 nm light is technically possible with this approach, and has been characterized experimentally, e.g., Tian et al. (2013) report an 11% reduction in measured NO_2 due to photodissociation from a 123 mW 405 nm LED.[1]

However, the 2B Model 405 instrument uses a sufficiently low-power 405 nm LED (4.3 mW) that photodissociation is expected to be minimal (< 1%).[2] Additionally, sampling artifacts due to NO_y species (specifically HONO and NO_3) and other possibly interfering compounds (e.g., glyoxyl and methyl glyoxyl) are also expected to be minimal due to (i) absorption cross sections at 405 nm that are at least a factor of six lower than NO_2 and (ii) typically much lower ambient levels of these compounds compared to NO_x species.[2]

Air exchange rate measurements

The air exchange rate (AER) during the duration of each test was measured every ~5 hours by periodically injecting CO_2 as a tracer gas in a bedroom. A small CO_2 cylinder was connected to an electronically powered solenoid valve regulator and controlled by an electric timer to automatically inject CO_2 every 5 hours for 15 minutes, yielding a typical peak of ~1200 ppm. Indoor and outdoor CO_2 concentrations were measured using two CO_2 monitors (PP System SBA-5; ±20 ppm accuracy) located in the living room near the window, one sampling indoors and one sampling outdoors through a penetration in the acrylic window. The average AER during every 5-hour interval was estimated by linear regression of the left hand side of Equation S1 versus time.[3]

$$-\ln\frac{Y_{in,t}-Y_{out}}{Y_{in,t=0}-Y_{out}}=\lambda t \quad \text{(S1)}$$

where $Y_{in,t}$ and $Y_{in,t=0}$ are the indoor CO_2 concentrations (ppm) measured at time t and $t = 0$, respectively; Y_{out} is the average outdoor CO_2 concentration (ppm) during the decay period; and λ is the average AER (h^{-1}) during the ~5-hour decay period. In some cases, the AER was clearly not constant during the entire 5-hour period; in those cases, hourly estimates of AER were made from the resulting decay data.

Estimating uncertainty

The uncertainty in each AER estimate was first calculated using the relative standard errors of the regression coefficients from Equation S1 and the average manufacturer-reported accuracy of both indoor and outdoor CO_2 monitors (20 ppm) added in quadrature. In Method 1, the uncertainty in P_{NO2} was calculated by adding the relative standard error of P_{NOx} from the regression of Equation 5 in the main text, the instrument accuracy (1 ppb for both NO_2 and NO, 2 ppb for total NO_x) relative to the average outdoor concentration used in Equation 6 in the main text, and the relative uncertainty of the AER in quadrature. The uncertainty of k_{NO2} in Method 1 was estimated by adding the uncertainty in P_{NO2} and the relative standard error of the regression coefficient from Equation 8 in quadrature.

In Method 2, the relative uncertainty in the indoor NO_2 total loss rate for ($\lambda_t + k_{NO2}$) was calculated by combining the average relative accuracy of the instrument (1 ppb divided by the average NO_2 concentration) and the relative standard error of the regression coefficient from Equation 8 added in quadrature. The uncertainty in the estimate of k_{NO2} was then calculated by combining the uncertainty of the total loss rate constant and the AER uncertainties. Finally, the uncertainty in P_{NO2} was estimated by error propagation with a combination of relative uncertainties of total loss rate constants, AER, and the standard error of regression coefficients of P_{NO2} from Equation 10 (for Methods 2a and 2b) and k_{NO} from Equation 9 (Method 2b only).

Supplemental Results

Example test data with NO oxidative reactions

Another example of resulting data from 24 hours of alternating indoor and outdoor concentrations followed by a single artificial elevation and decay experiment is shown in Figure

S2. The AER during the decay period was 1.14±0.01 h^{-1} and ranged 0.53-0.82 h^{-1} during the rest of the ~24-hour monitoring period under natural conditions. Estimates of k_{NO2} and k_{NO} were again made from the decay period data using Equations 7 and 8 (Figure S2c and S2d), yielding estimates of 0.18±0.12 h^{-1} and 0.25±0.09 h^{-1}, respectively. Clearly, k_{NO} was greater than zero and the resulting average indoor NO concentration during the 24-hour measurement period was lower than the average outdoor NO concentration (1.8 ppb versus 4.2 ppb, respectively). Therefore, the decision criteria in Method 2b were applied to instead assume that indoor oxidative reactions with NO were not negligible and therefore G_{NO2} at each time step was estimated using Equation 11. Continuing with these assumptions, P_{NO2} was estimated to be 0.73±0.10 for this test case one-parameter regression with Equation 10 and prior estimates of k_{NO2} and AER as a function of time. Because the natural concentration changes were relatively low during the longer-term sampling period in this test, Method 1 could not be used to make reasonable estimates of P_{NOx} and k_{NOx} from the resulting data (i.e., $P_{NOx} < 1$ and $k_{NOx} > 0$ h^{-1}). However, P_{NOx} was estimated to be 0.80±0.15 using Equation 6 with the average ambient NO and NO_2 concentrations during the test period (4.2 and 10.7 ppb, respectively) and the assumption of $P_{NO} = 1$.

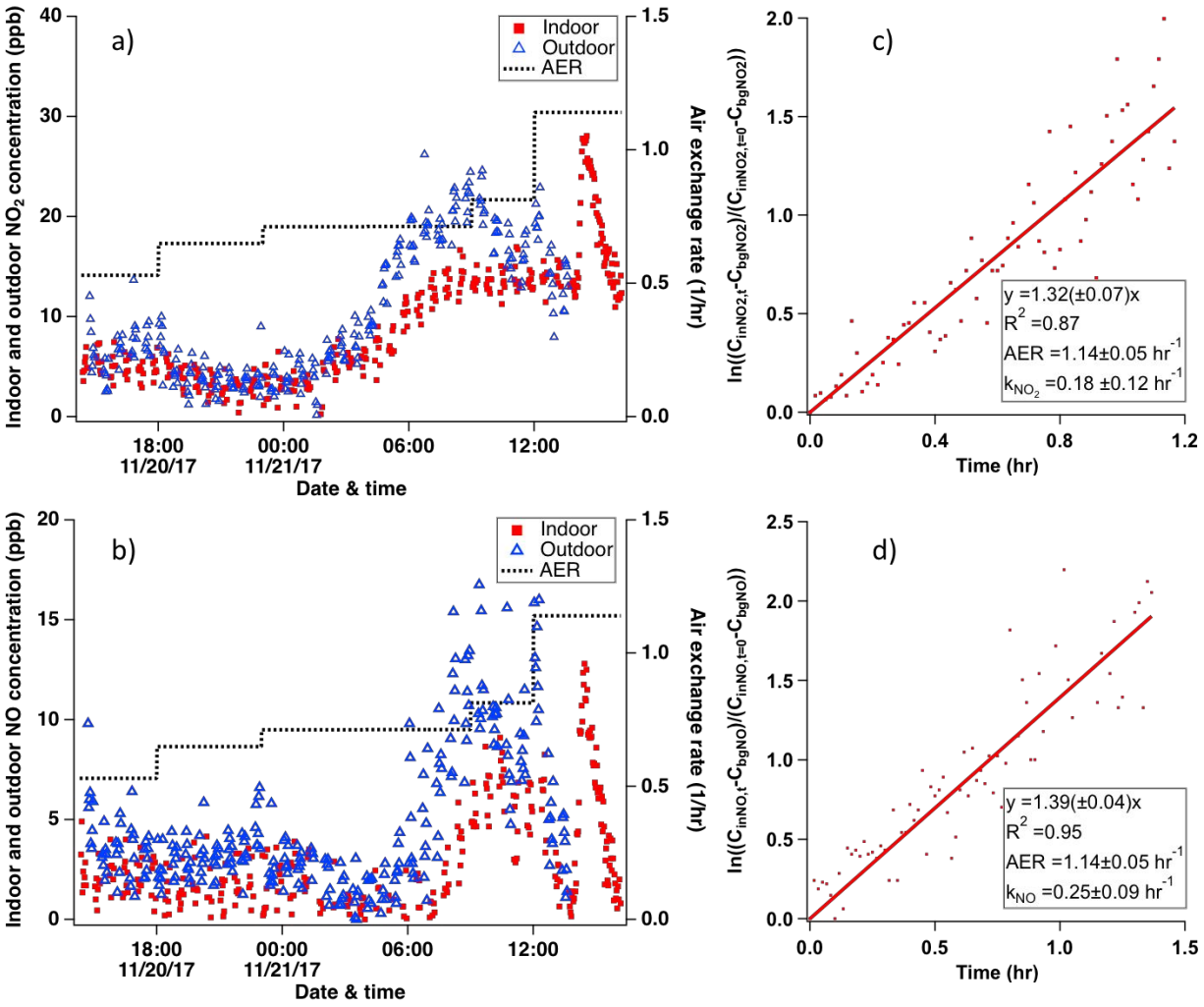

Figure S2. Example test data from a period of natural variations followed by a NO_x elevation and decay period (~14:00-15:00 on 11/21/17), with parameters estimated using Method 1 (failure) and Method 2b (success): (a) time-series indoor and outdoor NO_2 concentrations with 5-hour average AER overlaid, (b) time-series NO data from the same test period, (c) log-linear regression used to estimate the first order NO_2 decay rate constant, and (d) log-linear regression used to estimate the first order NO decay rate constant.

Distributions of P_{NOx} and k_{NOx} estimates and uncertainties

Figure S3 shows distributions of the parameter estimates and associated uncertainties for (a) NO_x penetration factor and (b) NO_x indoor loss rate from the 12 successfully completed tests, solved using a combination of Method 1 and 2 as appropriate. The mean (±s.d.) estimates of P_{NOx} solved by the natural elevation and decay approach (Method 1; n = 7), artificial elevation without indoor NO_2 generation via NO oxidation (Method 2a; n = 7), and artificial elevation with indoor

NO_2 generation via NO oxidation (Method 2b; n = 5) were 0.83±0.03, 0.85±0.04, and 0.82±0.05, respectively, ranging from 0.76 to 0.91 with an overall mean (±s.d.) of 0.84±0.13. Using Wilcoxon rank-sum tests, differences in estimates of P_{NOx} made using (i) Method 1 and Method 2 (lumping 2a and 2b together) and (ii) Method 1, Method 2a, and Method 2b (treated separately) were not statistically significant ($p > 0.05$). The mean (±s.d.) estimates of the relative uncertainty in P_{NOx} using Methods 1, 2a, and 2b were 12±1%, 15±1%, and 20±3%, respectively.

The mean (±s.d.) estimates of k_{NOx} solved by Method 1 (natural elevation), Method 2a (artificial elevation without indoor NO_2 generation via NO oxidation), and Method 2b (artificial elevation with indoor NO_2 generation by NO oxidation) were 0.04±0.03 h^{-1}, 0.04±0.01 h^{-1}, and 0.13±0.05 h^{-1}, respectively, ranging from 0.01 to 0.16 h^{-1} and with an overall mean (±s.d.) of 0.06±0.04 h^{-1} across all solution methods. The estimates of P_{NOx} and k_{NOx} were dependent on P_{NO2} and k_{NO2} as well as the ratios of ambient NO_2 and NO concentrations during each test. The mean (±s.d.) estimates of the relative uncertainty in k for NO_x made using Methods 1, 2a, and 2b were 85±77%, 45±29%, and 29±7%, respectively. Uncertainties in k_{NOx} were higher using primarily because of the smaller values of k_{NOx} (absolute uncertainties were similar across each method).

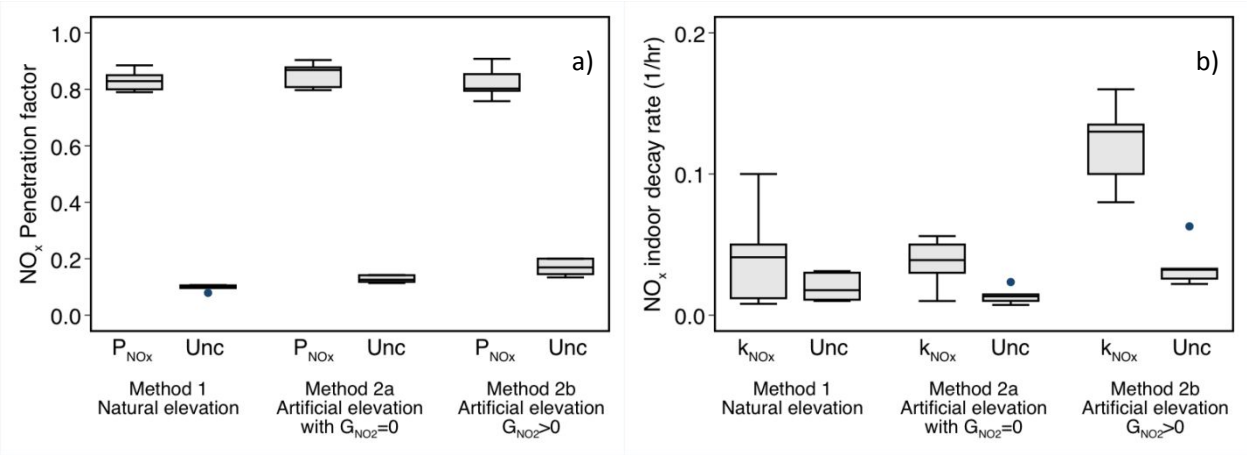

Figure S3. Parameter estimates and absolute uncertainties (labeled "Unc") made using three different methods for (a) NO_x penetration factor and (b) NO_x indoor loss rate. Boxes represent 25th, 50th, and 75th percentiles. Whiskers represent upper and lower adjacent values (1.5 times the differences between the 25th and 75th percentiles) and dots are outlier values.

Accuracy of solution methods

In order to explore the accuracy of estimates solved using the two test methods and variants of solution approaches, Figure S4 shows estimates of indoor NO_2 and NO_x concentrations for each time interval of each test (lumping all tests together) that were made using estimates of P_{NO2}, k_{NO2}, P_{NOx}, and k_{NOx} resulting from application of Method 1 (Figures S4a and S4c; n = 7 tests) and Method 2a and 2b combined (Figures S4b and S4d; n = 12 tests) plotted versus measured indoor NO_2 and NO_x concentrations at the same time intervals. The regression slopes of estimated versus measured NO_2 concentrations were 0.97 for Method 1 and 0.96 for Method 2, with R^2 values of 0.91 and 0.92, respectively. Therefore, both methods resulted in relatively accurate and repeatable estimates for P_{NO2} and k_{NO2}, albeit with a small negative bias that was perhaps caused by some of the simplifying assumptions we made for k_{NO2} and G_{NO2}. Similarly, the regression slopes of estimated versus measured NO_x concentrations were 0.99 for Method 1 and 0.99 for Method 2, with R^2 values of 0.99 and 0.99, respectively. Therefore, both Method 1 (directly applying two parameter regression fit to estimate P_{NOx}) and Method 2 (back-calculating P_{NOx} using the assumption of $P_{NO} = 1$ and P_{NO2} estimated separately, weighted by the average outdoor NO_2 and NO concentrations during testing) also resulted in relatively accurate and repeatable estimates for P_{NOx} and k_{NOx}.

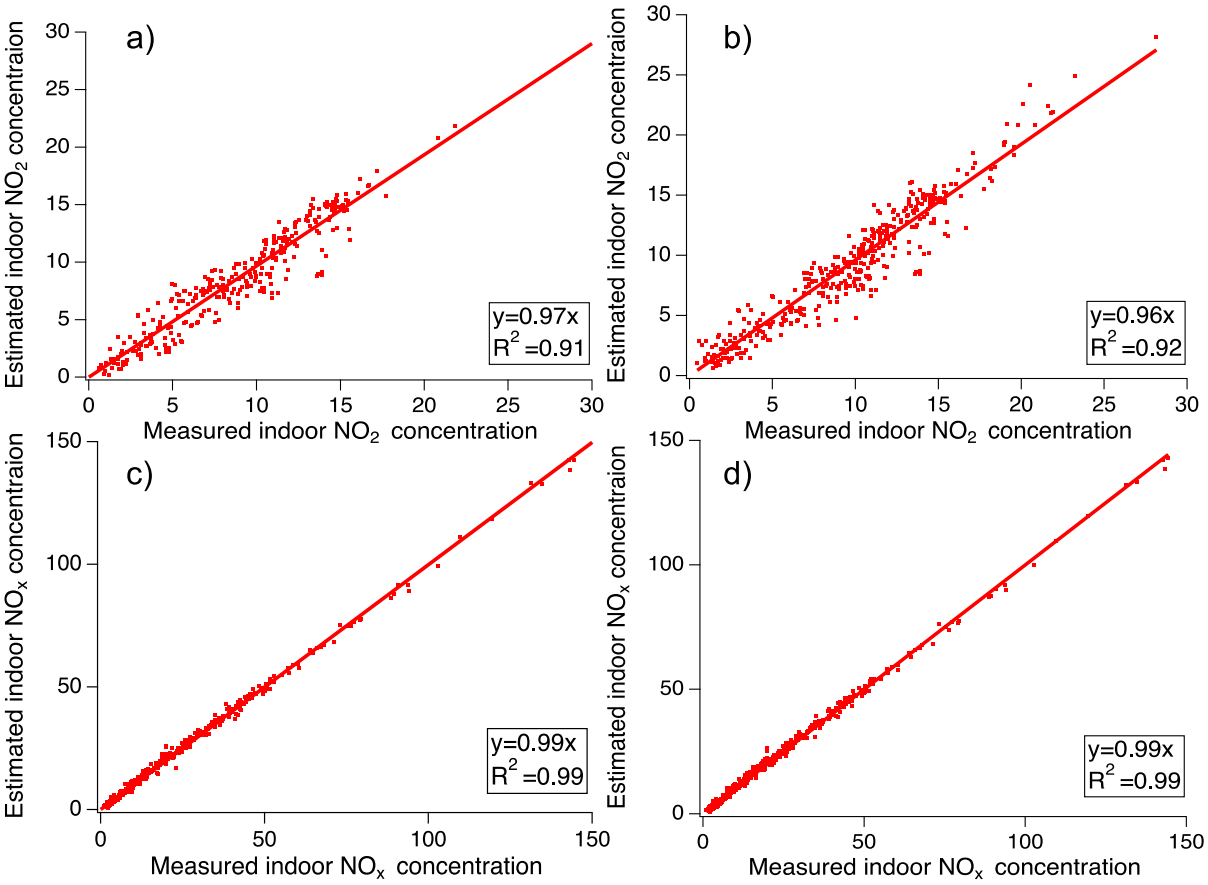

Figure S4. Plots of estimated indoor concentrations versus measured indoor concentrations for (a) NO_2 solved by Method 1, (b) NO_2 solved by Method 2a or 2b, (c) NO_x solved by Method 1, and (d) NO_x solved by Method 2a or 2b.

Influence of indoor environmental and ambient conditions

Table S1 shows several potentially influential indoor and outdoor environmental factors that were gathered for subsequent analysis, including averages of indoor and outdoor temperature and relative humidity, outdoor ozone concentrations, and wind speed and direction during the tests. Outdoor temperature, relative humidity (RH), and wind speeds and directions at 5-min intervals were gathered from a publicly accessible weather station on the Illinois Institute of Technology campus.[4] Outdoor ozone concentrations were taken at 1-hour intervals from the closest EPA regulatory monitoring site approximately 10 km to the west of the test site.[5] Unfortunately ozone instrumentation was not deployed on-site during the majority of our tests; however, Figure S5

shows a strong correlation between outdoor ozone concentrations measured immediately outside of the test apartment unit in a previous study[6] and ambient ozone concentrations reported at the closest regulatory monitoring site ($R^2 = 0.81$).

Table S1. Summary of average indoor and outdoor environmental conditions during test periods

	Indoor			Outdoor					
Date	Temp (℃)	RH (%)	Humidity ratio (g/g)	Temp (℃)	RH (%)	Humidity ratio (g/g)	Wind speed (mph)	Wind direction (from North)	O_3 (ppb)
2018/9/26	28.4	35.6	0.00854	15.6	58.4	0.00638	1.73	270	15
2018/9/12	29.1	47.1	0.01180	20.5	74.6	0.01098	6.8	22.5	28
2018/8/23	31.7	35.3	0.00982	22.2	51.3	0.0085	1.9	292.5	13
2018/3/12	27.3	16.6	0.00373	0.7	65.5	0.00262	6.2	145	32
2017/12/13	19.2	16.7	0.00229	-3.6	57.2	0.00167	6	90	12
2017/12/12	19.6	25.8	0.00365	1.6	75.9	0.00321	5.9	112.5	11
2017/12/1	25.4	22.5	0.00453	7.9	52.2	0.00344	3	90	9
2017/11/29	26.1	24.1	0.00498	8.2	58.3	0.00388	9.4	270	18
2017/11/20	16.3	37.3	0.00429	5.9	57.8	0.00333	6.65	112.5	22
2017/11/9	24.53	25.66	0.00500	3.5	66.1	0.00321	4.79	270	14
2017/10/25	24.4	35.7	0.00682	11.7	62	0.00526	7.5	270	12
2017/10/19	19.7	49.4	0.00698	15.8	56.1	0.00618	3	90	27
Mean	24.7	35.3	0.00709	11.6	62.0	0.00599	4.26	165	17.8

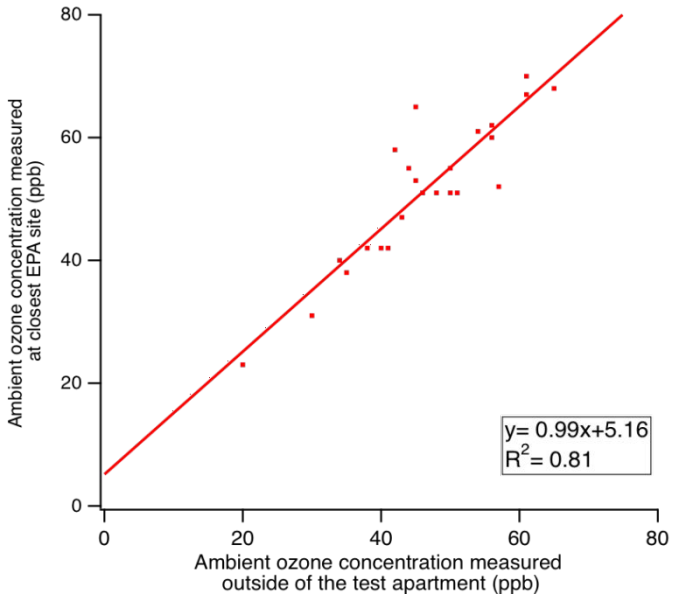

Figure S5. Ambient ozone concentrations measured immediately outside the test apartment in a previous study versus ambient ozone concentration measured at the closest EPA regulatory monitoring site approximately 10 km to the west

Supplemental References

(1) Tian, G.; Moosmüller, H.; Arnott, W. P. Influence of Photolysis on Multispectral Photoacoustic Measurement of Nitrogen Dioxide Concentration. *Journal of the Air & Waste Management Association* **2013**, *63* (9), 1091–1097. https://doi.org/10.1080/10962247.2013.790323.

(2) Birks, J. W.; Andersen, P. C.; Williford, C. J.; Turnipseed, A. A.; Strunk, S. E.; Ennis, C. A.; Mattson, E. Folded Tubular Photometer for Atmospheric Measurements of NO₂ and NO. *Atmos. Meas. Tech.* **2018**, *11* (5), 2821–2835. https://doi.org/10.5194/amt-11-2821-2018.

(3) ASTM E 741. Standard Test Method for Determining Air Change in a Single Zone by Means of a Tracer Gas Dilution. 2006.

(4) Illinois Tech Weather | Personal Weather Station: KILCHICA534 by Wunderground.com | Weather Underground https://www.wunderground.com/personal-weather-station/dashboard?ID=KILCHICA534 (accessed Jan 13, 2019).

(5) AirData website File Download page https://aqs.epa.gov/aqsweb/airdata/download_files.html#Raw (accessed Jan 13, 2019).

(6) Zhao, H.; Stephens, B. A Method to Measure the Ozone Penetration Factor in Residences under Infiltration Conditions: Application in a Multifamily Apartment Unit. *Indoor Air* **2016**, *26* (4), 571–581. https://doi.org/10.1111/ina.12228.